Journal of Power Sources 193 (2009) 699–705

Contents lists available at ScienceDirect

Journal of Power Sources

journal homepage: www.elsevier.com/locate/jpowsour

Predictive control of solid oxide fuel cell based on an improved Takagi–Sugeno fuzzy model

Jie Yang[a,b], Xi Li[c,*], Hong-Gang Mou[b], Li Jian[a]

[a] School of Materials Science and Engineering, State Key Laboratory of Material Processing and Die & Mould Technology, Huazhong University of Science & Technology, Wuhan 430074, China
[b] School of Mechanical and Electronic Information, China University of Geosciences, Wuhan 430074, China
[c] Department of Control Science and Engineering, Key Laboratory of Education Ministry for Image Processing and Intelligent Control, Huazhong University of Science & Technology, 1037 Luoyu Road, Wuhan 430074, China

ARTICLE INFO

Article history:
Received 4 March 2009
Received in revised form 15 April 2009
Accepted 15 April 2009
Available online 23 April 2009

Keywords:
Solid oxide fuel cell (SOFC)
Takagi–Sugeno (T–S) fuzzy model
Model predictive control (MPC)

ABSTRACT

Thermal management of a solid oxide fuel cell (SOFC) stack essentially involves control of the temperature within a specific range in order to maintain good performance of the stack. In this paper, a nonlinear temperature predictive control algorithm based on an improved Takagi–Sugeon (T–S) fuzzy model is presented. The improved T–S fuzzy model can be identified by the training data and becomes a predictive model. The branch-and-bound method and the greedy algorithm are employed to set a discrete optimization and an initial upper boundary, respectively. Simulation results show the advantages of the model predictive control (MPC) based on the identified and improved T–S fuzzy model for an SOFC stack.

1. Introduction

The solid oxide fuel cell is a high- or intermediate-temperature fuel cell, which operates in the range 600–1000 °C. The SOFC system is generally considered to suit the generation of electricity and heat in industrial application. A high operating temperature allows internal reforming and improves the reaction kinetics [1]. However, the fuel cell can be damaged by high temperature due to thermal fatigue or thermal cracking. High temperature also affects the stack reliability and durability, and shortens the stack lifespan [2]. Therefore, thermal management that controls the operating temperature and reduces temperature fluctuation is very important for SOFC stacks.

Many offline model-based control methods have been established for fuel cells [3–9], but few papers deal with MPC based on online control. MPC has been an active field of research during the last three decades, and there have been numerous successful applications of MPC technology [10–12]. MPC [13,14] has a number of advantages in that it can handle multivariable system problems, allows operation states close to the constraints, is capable of awareness of the actuator limitations of the model-based control, etc. MPC consists of model prediction, receding horizon optimization, and online feedback correction [15]. The SOFC system is a nonlinear one, in which the parameters vary within an operating range, and an MPC algorithm can satisfy the requirements of a control strategy.

Some researchers have examined control methods and strategies in relation to the SOFC system. Jurado [16] built a predictive control model to achieve online control of an SOFC system, which used a fuzzy Hammerstein model identified by the input–output data. Wu et al. [17] applied a nonlinear model predictive control method in order to control the voltage and guarantee fuel utilization within a safe range. The nonlinear predictive controller was based on an improved radial basis function (RBF) neural network, and a genetic algorithm (GA) was used to optimize the parameters. Yang et al. [18] presented a nonlinear predictive control algorithm based on a T–S fuzzy model for a molten carbonate fuel cell stack.

In this study, an online nonlinear MPC scheme based on an improved T–S fuzzy model has been built to control the temperature within a safe range. This improved T–S fuzzy model could be identified by training data that were provided by a physical model from Ref. [19]. The control sequence could be discretized and optimization could be sought using a principle of the branch-and-bound method, and a greedy algorithm has been employed to set the initial upper boundary for the performance index [20]. The MPC algorithm met the requirements for an online temperature control strategy, and the simulation results reflected the more effective temperature control.

2. Structure of the MPC system for an SOFC

2.1. Temperature predictive control system

The frame of the nonlinear MPC system of an SOFC is shown in Fig. 1, which mainly consists of a controlled plant (SOFC stack), a

* Corresponding author. Tel.: +86 027 87540924; fax: +86 027 87540924.
E-mail address: lixi@hust.edu.cn (X. Li).

0378-7753/$ – see front matter © 2009 Elsevier B.V. All rights reserved.
doi:10.1016/j.jpowsour.2009.04.022

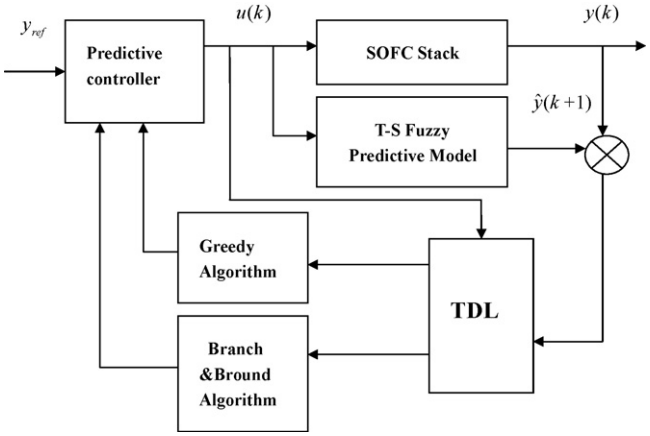

Fig. 1. The structure of the MPC system.

nonlinear improved T–S fuzzy predictive model, and a predictive controller. The SOFC physical model (see Appendix B) described in Ref. [19] was built with MATLAB to imitate the real 3.5 kW SOFC stack and is shown in Fig. 2. The physical model was constructed from the mass balance equations and the enthalpy balance equations. In addition, the MPC system also contained modules of the branch-and-bound algorithm, the greedy algorithm, and the tapped delay line (TDL). For the SOFC dynamic physical model, temperature was the controlled variable. Flow rates of hydrogen and air were chosen as manipulated variables, and the load current was considered as a disturbance.

In Fig. 1, y_{ref} is the reference curve of stack temperature, $u(k)$ is the manipulated variable, $y(k)$ is the current value of stack temperature, and $\hat{y}(k+1)$ is the predicted next value. The T–S fuzzy model predicts future stack temperature values on the basis of history stack temperature values. The optimal controller can determine the next control signal for the SOFC stack according to the difference between the next reference values and the predicted stack temperature values.

2.2. Predictive model based on an improved T–S fuzzy model

An improved T–S fuzzy model can be obtained by antecedent and consequent identification. The fuzzy rule is of the form "if... then...". The ith rule of the lth output $\hat{y}_{l,i}(k+1)$ is given by

$$R_{l,i}: \text{If } x(k) \text{ is } A_i^l, \text{ then}$$

$$\hat{y}_{l,i}(k+1) = p_{i,0}^l + p_{i,1}^l x_{k1} + \cdots + p_{i,n}^l x_{kn} \quad (i = 1, \ldots, c) \tag{1}$$

where $x(k)$ is the regression data vector consisting of input–output data at the kth instant and before, c is the number of rules, $A_i^l = \{A_{i,1}^l, \ldots, A_{i,n}^l\}$ is the set of membership functions associated with the ith rule, and $p_i^l = [p_{i,0}^l, p_{i,1}^l, \ldots, p_{i,n}^l]$ is the parameter vector of the ith submodel.

Antecedent identification is implemented by fuzzy clustering based on the principle of the fuzzy C-means (FCM) algorithm [21]. The consequent part of the fuzzy rule is identified by using the traditional linear identification method, the least-squares method.

The improved T–S fuzzy model is fundamentally different from the modified T–S fuzzy model in Ref. [19] because the latter is an offline model method whereas the former is an online model method. Offline models are sometimes made up of many control rules and the open-loop data that they generate do not cover all data needed for closed-loop control, hence it is difficult to obtain accurate predictive output with such models.

The specific algorithm and formula of the improved T–S model is inferred as follows [21–25]:

(1) Initialization of the number of fuzzy clustering c (c is greater than 1), the clustering center vector $v_i = [v_{i1} \ldots v_{in}]$ ($i = 1, \ldots, c$), the fuzzy parameter m (m is greater than 1), the discarding index q (q is greater than 1), and the learning rate η (η is greater than 0).
(2) Assessment of whether there is a clustering center vector v_i in the q (discarding index) consecutive sampling period that satisfies the criterion that the distance from v_i to the consecutive input–output data vector is always the farthest. If so, a new center vector is adopted to replace v_i, for example, the current data vector $x(k)$.
(3) Calculation of the distance between $x(k)$ and each cluster center at the $(k-1)$th instant:

$$d_i'(k) = \sqrt{\sum_{j=1}^{n} [x_j(k) - v_{ij}(k)]^2}, \quad i = 1, \ldots, c \tag{2}$$

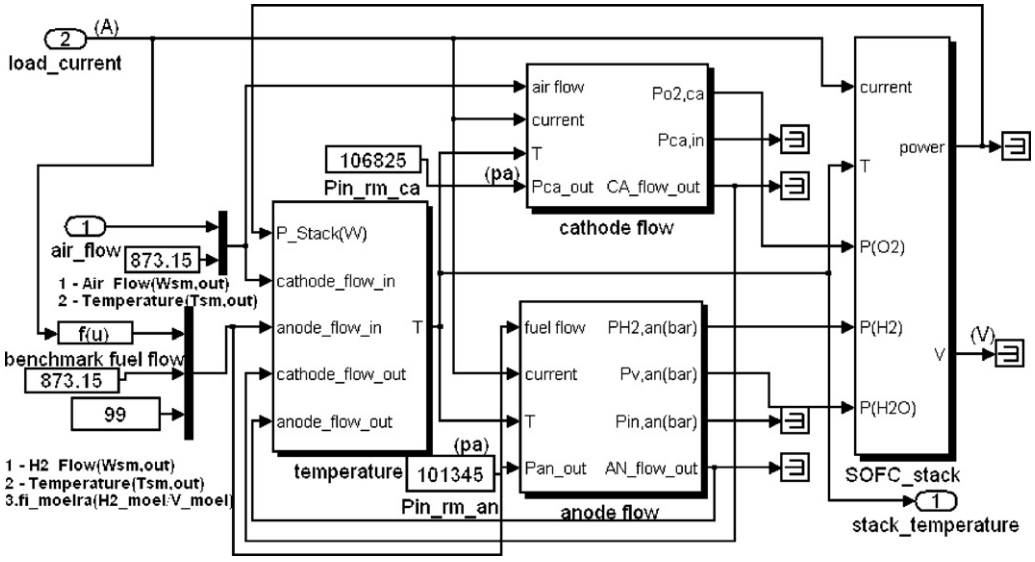

Fig. 2. The SOFC stack physical model.

and accumulating the number of clustering satisfying the criterion that the distance between each clustering center vector and the consecutive input–output data vector is always the farthest.

(4) Determination of the membership degree of $x(k)$ with respect to the ith clustering at the $(k-1)$th instant:

$$\mu_i'(k) = \left[\sum_{j=1}^{c}\left(\frac{d_i'(k)}{d_j'(k)}\right)^{(2/(m-1))}\right]^{-1}, \quad i = 1, \ldots, c \tag{3}$$

(5) Adjustment of the clustering center vector at the kth instant according to the membership degree of $x(k)$ with respect to the ith clustering at the $(k-1)$th instant:

$$v_i(k) = v_i(k-1) + \eta\mu_i'(k)^2[x(k) - v_i(k-1)] \tag{4}$$

(6) Calculation of the distance between $x(k)$ and each clustering center as well as the membership degree of $x(k)$ according to the new clustering center at the kth instant:

$$d_i(k) = \sqrt{\sum_{j=1}^{n}[x_j(k) - v_{ij}(k)]^2} \tag{5}$$

$$\mu_i(k) = \left[\sum_{j=1}^{c}\left(\frac{d_i(k)}{d_j(k)}\right)^{(2/(m-1))}\right]^{-1} \tag{6}$$

(7) Use of the least-squares recurrence method to identify the linear composition factors of consequence. The data vector $x(k) = [x_{k1}\ x_{k2}\ \ldots\ x_{kn}]$ is given. The output of the fuzzy model, $\hat{y}(k+1)$, is then calculated:

$$\begin{aligned}\hat{y}(k+1) &= \frac{\sum_{i-1}^{c}\omega_i[x(k)]\hat{y}_i(k+1)}{\sum_{i=1}^{c}\omega_i[x(k)]} \\ &= \sum_{i=1}^{c}\mu_i(k)\hat{y}_i(k+1) = \sum_{i=1}^{c}\mu_i(k)(p_{i0} + p_{i1}x_{k1} + \cdots + p_{in}x_{kn}) \\ &= \Phi(k) \times \theta\end{aligned} \tag{7}$$

where $\omega_i[x(k)]$ expresses expectance value,

$$\mu_i(k) = \frac{\omega_i[x(k)]}{\sum_{i=1}^{c}\omega_i[x(k)]}$$

$$\Phi(k) = [\mu_1\ \mu_2 \cdots \mu_c\ \mu_1 x_{k1}\ \mu_2 x_{k1} \cdots \mu_c x_{k1} \cdots \mu_1 x_{kn}\ \mu_2 x_{kn} \cdots \mu_c x_{kn}]$$

$$\theta = [p_{10}\ p_{20} \cdots p_{c0}\ p_{11}\ p_{21} \cdots p_{c1} \cdots p_{1n}\ p_{2n} \cdots p_{cn}]^T$$

The least-squares recurrence algorithm is employed to identify θ in order to minimize the total cumulative square-root error between the actual output and the model output.

(8) If the control process does not end, $k = k-1$, it returns to Step 2.

Completion of the above modeling process leads to a nonlinear improved T–S fuzzy predictive model.

3. Discrete optimization of control variables

MPC consists of the identified predictive model, the objective function, and all kinds of constraints of the system variables [26]. MPC must find a control sequence in the future limited horizon so that the objective function is minimized, and the first control variable of a control sequence is imposed on the controlled objective in order to achieve so-called receding horizon optimization control.

In this study, the nonlinear predictive control algorithm for optimization is described as follows. The task is to search for an optimal control sequence $U(k)$ $(=[u(k)\,u(k+1)\ldots u(k+M-1)])$ that satisfies the condition that the objective function is minimized on the basis of the fuzzy predictive model, the prediction horizon P, the control horizon M $(M \le P)$, and the regression data vector $x'(k)$ consisting of input–output data at the current instant and before:

$$x'(k) = [u(k-1), \ldots, u(k-n_u), y(k), \ldots, y(k-n_y)] \tag{8}$$

Here, the quadratic objective function J is employed:

$$J = \sum_{i=1}^{P} q_i[y(k+i) - y_m(k+i)]^2 + \sum_{j=1}^{M} r_j \Delta u^2(k+j-1) \tag{9}$$

where q_i and r_j are weight coefficient, from the every time k, there are j control increments $\Delta u(k), \ldots, \Delta u(k+j-1)$, $y(k+i)$ is actual output, and $y_m(k+i)$ is model predictive output. The constraints on the system variables can be confirmed according to different system requirements. The discrete optimization of the control sequence employs a branch-and-bound algorithm, which is an integral part of the programming. The basic concept of obtaining the optimal solution is to divide the feasible solution space into a number of small subspaces, and then to select the appropriate upper and lower boundary functions for narrowing the solution scope until the optimal solution is obtained [8,21–25].

3.1. Determining the tree structure discrete search space of the control sequence U(k)

The error $e(k)$ between the objective setting value $y_r(k)$ of the current sampling period and the actual system output $y(k)$, and the error change ratio $ec(k)$, may be calculated as follows:

$$e(k) = y_r(k) - y(k) \tag{10}$$

$$ec(k) = e(k) - e(k-1) \tag{11}$$

e and ec are discretized into E and EC in their respective fuzzy domains, and the variable $du(k)$ of $u(k)$ is inferred according to the following analytical fuzzy reasoning formula:

$$du(k) = \alpha E + (1-\alpha)EC \tag{12}$$

where α is an undetermined coefficient.

The consecutive space of $u(k)$ that is centered on $u(k-1)$ is given by

$$B = (u(k-1) - abs(du), u(k-1) + abs(du)) \tag{13}$$

The consecutive space of $u(k)$ is then discretized into the discrete search space. Analogously, the discrete search space of $u(k+i)$ can be obtained according to $y_r(k+i)$ and $\hat{y}(k+i)$ in the control horizon $(1 \le i \le M-1)$ based on each discrete search point of $u(k+i-1)$. The control sequence does not branch anymore during the sampling period beyond the control horizon $(M \le i \le P-1)$. Fig. 3 illustrates the discrete search space of tree structure of the control sequence $U(k)$ in the predictive horizon P and the control horizon M. In this figure, $u_t(k+i)$ $(t = 1, \ldots, n_{k+1})$ denotes the tth discrete search point in the discrete space of u at the $(k+i)$th sample instant. This algorithm embodies the branch principle of the branch-and-bound method [19].

3.2. Searching for the optimal control sequence

The process of searching for the optimal control sequence $U(k)$ is shown in Fig. 3. In the discrete search space of tree structure, searching for an optimal control sequence means meeting the criterion that the quadratic objective function is minimized. Firstly,

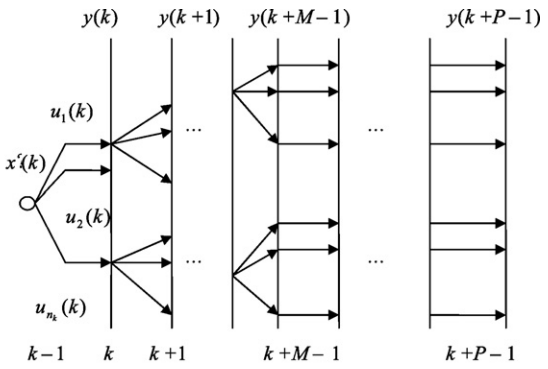

Fig. 3. The tree structure discrete searching space of control sequence $U(k)$.

the greedy algorithm is employed to find a good solution in order to set the initial upper boundary for the performance index [27].

It is then assumed that $u(k+i-1)$ has been given. The performance indices of all discrete control variables $u_t(k+i)$ $(t=1,\ldots,n_{k+1})$ are calculated at the $(k+i)$th $(i=1,\ldots,P-1)$ level according to Fig. 3:

$$J_t(k+i) = q_i[y_r(k+i) - y_t(k+i)]^2 + r_i[u_t(k+i) - u(k+i-1)]^2 \tag{14}$$

The minimum of the quadratic objective function as well as $u(k+i)$ can be expressed as follows:

$$J_{\min}(k+i) = \min_t\{J_t(k+i)\} \tag{15}$$

J_{upper} is the initial upper boundary of performance index for searching for the optimal control sequence and it can be calculated by the following formula:

$$J_{upper} = \sum_{i=0}^{P-1} J(k+i) \tag{16}$$

The process of searching for the optimal control sequence $U(k)$ is shown in Fig. 4. The notation in the following steps corresponds with that in Fig. 4.

(1) It is assumed that $u_t(k+i)$ $(i=1,\ldots,P-1)$ is based on $u(k+i-1)$ and J is calculated as follows:

$$J = \sum_{l=k}^{k+i} q_l[y_r(l) - y(l)]^2 + \sum_{l=k}^{\min\{M,k+i\}} r_l \Delta u(l)^2 \tag{17}$$

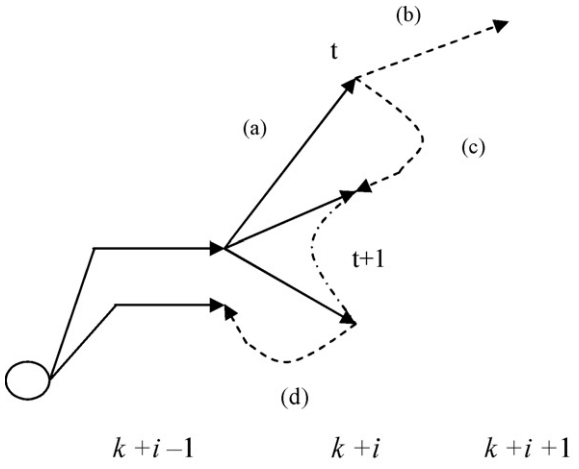

Fig. 4. Demonstration of the searching process.

(2) While J is less than J_{upper}, the process will continue from $u(k+i+1)$ to $u(k+P-1)$ on the basis of $u_t(k+i)$; J is assigned to J_{upper} ($J_{upper}=J$) if J is still less than J_{upper} in the process.
(3) When J is greater than J_{upper}, the latter subspaces with respect to $u_t(k+i)$ are eliminated and $u_{t+1}(k+i)$ is reselected.
(4) If $t=n_{ki}$, $u(k+i+1)$ must be reselected.

In this way, the entire space is searched and the optimal control sequence $U(k)$ with respect to the minimum J is found. The first-dimension element $u(k)$ of $U(k)$ is regarded as a control variable for the next sampling period and is applied to the controlled objective so that a new sampling output value $y(k+1)$ is obtained. When the new input–output data vector $x(k)$ is restructured, it is applied to receding horizon optimization control of the next circulation.

4. Simulation results

This section presents numerical simulations to illustrate the validation of the proposed predictive control developed for the temperature of SOFC stack based on an improved T–S fuzzy model. From

Table 1
Parameters of the SOFC stack used in the physical model.

Item	Value
Cell number	60
Cell active area (m^2)	0.01
Heat capacity per cell area ($J\,K^{-1}\,m^{-2}$)	7000
Arm power (kW)	3.5
Anode total volume (m^3)	0.005
Cathode total volume (m^3)	0.001
Gas inlet flow constant	0.3629×10^{-5}
Anode gas outlet flow constant	0.0544×10^{-5}
Cathode gas outlet flow constant	0.2118×10^{-5}
Air heat capacity ($J\,kg^{-1}\,K^{-1}$)	1004
Air density ($kg\,m^{-3}$)	1.23
Oxygen density ($kg\,m^{-3}$)	1.36
Nitrogen density ($kg\,m^{-3}$)	1.19
Air gas constant ($kg\,m^{-3}$)	286.9
Oxygen gas constant ($kg\,m^{-3}$)	259.8
Nitrogen gas constant ($kg\,m^{-3}$)	296.8
Hydrogen gas constant ($kg\,m^{-3}$)	4.1243×10^{3}
Oxygen molar mass ($kg\,mol^{-1}$)	0.032
Nitrogen molar mass ($kg\,mol^{-1}$)	0.028
Hydrogen molar mass ($kg\,mol^{-1}$)	2.016×10^{-5}
Faraday's constant	96485.34
Universal gas constant ($kg\,m^{-3}$)	8.31451

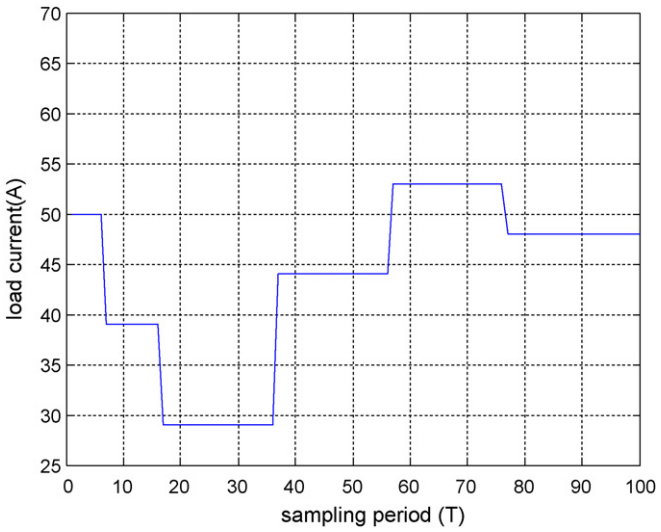

Fig. 5. Load current curve.

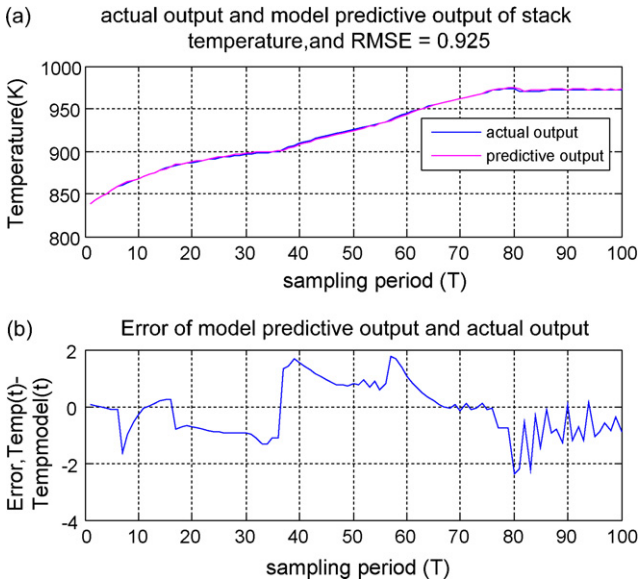

Fig. 6. Tracking curves and error of actual output and model predictive control.

above-mentioned Sections 2 and 3, the model predictive control is designed based on the improved T–S model which is set up at first. The SOFC physical model (see Appendix B) described in Ref. [19] is used to obtain the input/output data, and just replaces the true SOFC stack. In this study, the training data is generated with the physical SOFC model. In order to obtain available identification data, the input signals of the SOFC physical model were uniformly random, mainly is the current (0–60 A). The parameters of a 3.5 kW SOFC stack were used in the simulation, and are given in Table 1. The input/output data was collected from the simulation, and then the fuzzy modeling algorithm was employed to identify the T–S fuzzy model. To validate the improved T–S fuzzy model, it was used to perform dynamic simulation of the SOFC stack. The SOFC stack temperature had to be kept constant (in general 973.15 K). The initialization parameters of the improved T–S model were as follows: number of fuzzy clustering $c = 4$, fuzzy parameter $m = 3$, and learning rate $\eta = 0.2$. Simulations were performed for all the schemes with the following tuning parameters of the predictive controller: prediction horizon $P = 14$, control horizon $M = 3$, controlled variable weighting $r = 0.2$. The load current was considered as a disturbance, as shown in Fig. 5. Tracking curves and the deviation between the actual output and the model predictive output of the stack temperature are shown in Fig. 6. The deviation between the actual output and the model predictive control fluctuates within ±2 K and the MPC control strategy displays good control accuracy. Fig. 7 shows that the SOFC stack is controlled by the nonlinear predictive control algorithm based on the improved T–S fuzzy model. MPC adjusts the operating temperature to the set value (973.15 K), minimizes the temperature fluctuation, and provides control with satisfactory effectiveness.

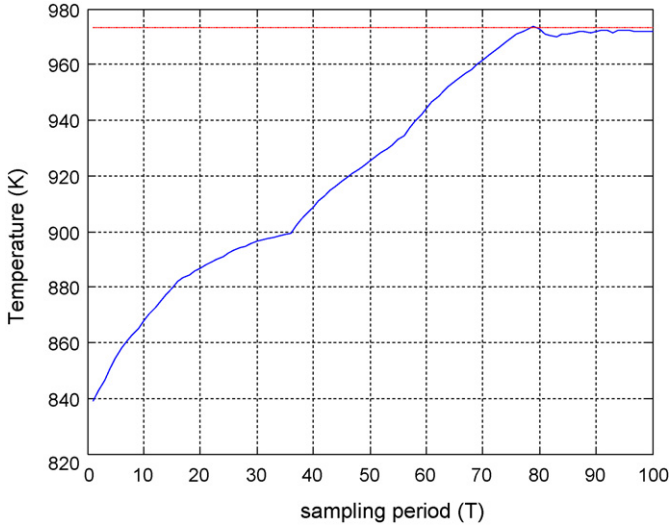

Fig. 7. Response of model predictive control.

5. Conclusions

Thermal management of SOFC stacks is very important because high temperature and temperature fluctuation can lead to serious problems. In this study, a nonlinear MPC algorithm based on a T–S fuzzy identification model has been proposed. Simulation results have shown the MPC method to be valid and that it gives good performance by virtue of the nonlinear predictive controller.

It is clear that a model of a nonlinear SOFC stack can be built on the basis of an improved T–S fuzzy model, and that this can be used to predict the temperature responses online. The stack temperature can be controlled so as to smoothly maintain the set value, and the simulation results show the nonlinear predictive controller to be superior for this purpose.

Acknowledgments

This research has been financially supported by the National Science Foundation of China (60804031), the “863” High-Tech Project (2006AA05Z148), and the Key Laboratory of Education Ministry for Image Processing and Intelligent Control (200701).

Appendix A. Nomenclature

A	cell active area (m^2)
C_p	specific heat capacity of gas species ($J\,mol^{-1}\,K^{-1}$)
$\dot{C}_p$	area specific heat capacity ($J\,K^{-1}\,m^{-2}$)
F	Faraday's constant (96,485 $C\,mol^{-1}$)
H	enthalpy (J)
$\dot{H}$	enthalpy flow (W)
h	specific enthalpy ($J\,mol^{-1}$)
I	current (A)
i	current density ($A\,m^{-2}$)
i_0	exchange current density ($A\,m^{-2}$)
i_r	reaction current density ($A\,m^{-2}$)
m	mass (kg)
N	molar flux ($mol\,m^{-2}\,s^{-1}$)
n	number of moles (mol)
$\dot{n}$	molar flow ($mol\,s^{-1}$)
n_i	molar number of species i (mol)
$\dot{n}^c$	hydrogen combustion molar flow ($mol\,s^{-1}$)
P	pressure (bar)
R	universal gas constant (8.314 $J\,mol^{-2}\,K^{-2}$)
T	temperature (K)
T_0	ambient temperature (K)
t	time (s)
U	voltage (V)
V	volume (m^2)
x	input vector
x_i	molar fraction of species
y	output vector

Greek letters

α	symmetry factor, learning factor
β	a T–S factor
ν	stoichiometric coefficient
η	overpotential (V)

Subscripts

i	gas species i
r	reaction

Superscripts

in	fuel cell inlet
out	fuel cell outlet

Appendix B. A physical model of an SOFC stack

In this SOFC physical model, some simplifications and assumptions are made, since high accuracy is not necessary for a physical model that serves for a subsequent control strategy. Any deviations between the model and the real fuel cell can be managed by a feedback loop in the control system [28]. This section has many symbols which can be defined in Appendix A. The proposed SOFC stack physical model has the following assumptions:

(1) Stack is fed with hydrogen and air; the fuel processor dynamics are not included.
(2) A uniform gas distribution among the cells is assumed, since there is a small deviation of the gas distribution.
(3) There is no heat transfer among the cells. Each cell has the same temperature and current density.
(4) There is no heat exchange between the stack and the ambient environment.
(5) The channels that transport gases along the electrodes have a fixed volume and small dimension, so there is a constant pressure in the stack.

B.1. Mass balance model

For a generic species i, the dynamic mole balance is

$$\frac{dn_i}{dt} = \dot{n}^{in}x_i^{in} - \dot{n}^{out}x_i + \nu_i\frac{i_rA}{F} \tag{B.1}$$

The stoichiometric factor ν_i indicates how many moles of the species are produced or consumed for each mole of electrons transferred. The anodic and cathodic reactions in the SOFC are, respectively:

$$H_2 + O^{2-} \rightarrow H_2O + 2e^-$$

$$1/2O_2 + 2e^- \rightarrow O^{2-} \tag{B.2}$$

then $\nu_{O_2} = -1/2$, $\nu_{H_2} = -1$, $\nu_{H_2O} = 1$, and $\nu_{N_2} = 0$.

According to the Butler–Volmer equation [29]:

$$i_r = i_0(e^{\alpha(nF/RT)\eta} - e^{-(1-\alpha)(nF/RT)\eta}) \tag{B.3}$$

When pressure is constant, the total outlet molar flow depends only on the transient reaction rate and temperature and can be calculated using the following relation:

$$\dot{n}^{out} = \dot{n}^{in} + \sum_i \nu_i\frac{i_rA}{F} + \frac{pV}{RT^2}\frac{dT}{dt} \tag{B.4}$$

The term $\sum_i \nu_i(i_rA/F)$ represents the algebraic sum of gas reaction molar flow, and $(pV/RT^2)\,(dT/dt)$ reflects thermal expansion. Inserting Eq. (B.4) into Eq. (B.1) and assuming constant pressure, the molar balance becomes:

$$\frac{pV}{RT}\frac{dx_i}{dt} = \dot{n}^{in}(x_i^{in} - x_i) + \frac{i_rA}{F}\left(\nu_i - x_i\sum_j \nu_j\right) \tag{B.5}$$

B.2. Energy balance model

Here only the enthalpy balance is considered. The main sources and sinks of heat for an SOFC are entering and exiting flow, the heat generated by cell reactions, and the heat lost to the environment. An enthalpy balance equation yields:

$$\frac{dH}{dt} = \dot{H}^{in} - \dot{H}^{out} - i_rVA - \dot{H}^{loss} \tag{B.6}$$

The term i_rVA represents the electrical power generated. The relationship between enthalpy and temperature can be expressed as:

$$\frac{dH}{dt} = A\dot{c}_p\frac{dT}{dt} \tag{B.7}$$

The entering enthalpy flow also contains the heat generated by the combustion of hydrogen, hence the total entering enthalpy flow is equal to the enthalpy associated with the ambient air plus the entering hydrogen flow:

$$\dot{H}^{in} = \dot{n}_{air}h_{air}(T_0) + (\dot{n}_{H_2} + \dot{n}^c_{H_2})h_{H_2}(T_{H_2}) \tag{B.8}$$

For simplification $T_{H_2} = T_0$ is assumed without causing any meaningful deviation.

The total outlet molar flow will be larger than or equal to the entering one and the expression of this is

$$\dot{H}^{out} = \sum_i \dot{n}_i^{out}h_i(T) \tag{B.9}$$

and the outlet molar flow for species i, $\dot{n}_i^{out}$ can also be expressed as:

$$\dot{n}_i^{out} = \dot{n}_i^{in} + \nu_i\left(\dot{n}^c_{H_2} + \frac{i_rA}{2F}\right) + x_i\frac{pV}{RT^2}\frac{dT}{dt} \tag{B.10}$$

where $\dot{n}_i^{in}$ is the entering molar flow, $\nu_i(\dot{n}^c_{H_2} + (i_rA/2F))$ is the molar flow associated with hydrogen reaction and combustion, and the term $x_i\,(pV/RT^2)\,(dT/dt)$ is related to gas thermal expansion. For the sake of simplicity, it is assumed that $\dot{H}^{loss} = 0$ [28].

B.3. Temperature control dynamic model

Having assumed that temperature is uniform in a stack, Eq. (B.6) determines its dynamics. According to simultaneous Eqs. (B.6) and (B.7), it can be obtained that

$$\begin{aligned} A\dot{c}_p\frac{dT}{dt} &= \dot{H}^{in} - \dot{H}^{out} - i_rVA \\ &= (\dot{H}^{in}(T) - \dot{H}^{out}(T)) - (\dot{H}^{in}(T) - \dot{H}^{in}(T_0)) - i_rVA \end{aligned} \tag{B.11}$$

The terms $(\dot{H}^{in}(T) - \dot{H}^{out}(T))$ and $(\dot{H}^{in}(T) - \dot{H}^{in}(T_0))$, respectively, represent the reaction heat and the sensible heat.

In Eq. (B.11) it assumed that the specific heat capacity for all the species is approximately the same on condition that the pressure is constant. This is adequate for the control-oriented modeling. According to Eq. (B.11), the temperature control model can be built with MATLAB.

B.4. Temperature control model realization in MATLAB

This physical MATLAB model has two input variables, air flow and H_2 flow, and one output variable, *T*. A virtual 3.5 kW SOFC stack is used in the simulation. The stack consists of 60 cells with anode and cathode gases in cross-flow and cell active area 0.01 m^2. The physical model replaces the real SOFC stack to generate the simulation data required for the modified T–S fuzzy model. The enthalpy expressions can be acquired from the published literature [30] and the relationship between enthalpy and temperature for different gases is reflected in these expressions. The Enthalpy_out block and Enthalpy_in block can be expressed as follows (*w* expresses molar flow):

For Enthalpy_in block:

$$h\_in = w\_\text{air} \times h\_\text{air} + w\_H_2 \times h\_H_2 + w\_V \times h\_V \quad \text{(B.12)}$$

where

$$h\_\text{air} = -1.0947\,e4 + 32.50T\_\text{air}$$

$$h\_H_2 = -0.9959\,e4 + 30.73T\_\text{fuel}$$

$$h\_V = -25.790\ e4 + 42.47T\_\text{fuel} \quad \text{(B.13)}$$

$$w\_H_2 = w\_\text{fuel} \times fi\_\text{moelra} \times 2.016/(fi\_\text{moelra} \times 2.016 + 18.02)$$

$$w\_V = w\_\text{fuel} - w\_H_2 \quad \text{(B.14)}$$

For the Enthalpy_out block:

$$h\_\text{out} = w\_O_2 \times h\_O_2 + w\_N_2 \times h\_N_2 + w\_H_2 \times h\_H_2 + w\_V \times h\_V \quad \text{(B.15)}$$

and

$$h\_O_2 = -1.2290\,e4 + 35.12T$$

$$h\_N_2 = -1.0590\,e4 + 31.40T$$

$$h\_H_2 = -0.9959\,e4 + 30.73T$$

$$h\_V = -25.790\ e4 + 42.47T \quad \text{(B.16)}$$

Based on the physical model, it can be established that the load signal change can vary the SOFC stack temperature.

References

[1] W. Sangtongkitcharoen, S. Vivanpatarakij, N. Laosiripojana, A. Arpornwichanop, S. Assabumrungrat, Chem. Eng. J. 138 (2008) 436–441.
[2] P. Aguiar, C.S. Adjiman, N.P. Brandon, J. Power Sources 147 (2005) 136–147.
[3] J. Arriagada, P. Olausson, A. Selimovic, J. Power Sources 112 (2002) 54–60.
[4] F. Jurado, J. Power Sources 154 (2006) 145–152.
[5] H.-B. Huo, X.-J. Zhu, G.-Y. Cao, J. Power Sources 162 (2006) 1220–1225.
[6] Y.-W. Kang, J. Li, G.-Y. Cao, H.-Y. Tu, J. Li, J. Yang, J. Power Sources 179 (2008) 683–692.
[7] F. Yang, X.-J. Zhu, G.-Y. Cao, J. Power Sources 166 (2007) 354–361.
[8] Z.-D. Zhong, X.-J. Zhu, G.-Y. Cao, J. Power Sources 160 (2006) 293–298.
[9] A. Saengrung, A. Abtahi, A. Zilouchian, J. Power Sources 172 (2007) 749–759.
[10] J. Richalet, Automatica 29 (1993) 1251–1274.
[11] S.J. Qin, T.A. Badgwell, Proceedings of the Fifth International Conference on Chemical Process Control, 1997, pp. 232–256.
[12] S. Mollov, R. Babuska, J. Abonyi, H. Verbruggen, IEEE Trans. Fuzzy Syst. 12 (2004) 661–675.
[13] C.E. Garcia, D.M. Prett, M. Morari, Automatica 25 (1991) 335–348.
[14] E. Katende, A. Jutan, Ind. Eng. Chem. Res. 35 (1996) 3539–3546.
[15] G. Wei, H. Min, Proceedings of 2006 American Control Conference Minneapolis, MN, USA, June 14–16, 2006, pp. 1569–1574.
[16] F. Jurado, J. Power Sources 158 (2006) 245–253.
[17] X.-J. Wu, X.-J. Zhu, G.-Y. Cao, H.-Y. Tu, J. Power Sources 179 (2008) 232–239.
[18] F. Yang, X.-J. Zhu, G.-Y. Cao, W.-Q. Hu, J. Power Sources 183 (2008) 253–256.
[19] J. Yang, X. Li, H.-G. Mu, J. Li, J. Power Sources 188 (2009) 475–482.
[20] G.E. Tsekouras, Adv. Eng. Software 36 (2005) 287–300.
[21] B. Liu, Ph.D. Thesis, Zhejiang University, 2004.
[22] H.-W. Wang, G.-F. Ma, Z.-C. Wang, Aeronaut. Trans. 20 (1999) 239–241.
[23] L.-X. Wang, Adaptive Fuzzy Systems and Control: Design and Stability, National Defense Industrial Publishing Company, Beijing, 1995.
[24] L.-X. Wang, Adaptive Fuzzy Systems and Control: Design and Stability, Prentice-Hall, Englewood Cliffs, NJ, 1994.
[25] X. Li, Ph.D. Thesis, Shanghai Jiaotong University, 2005.
[26] N.L. Ricker, Proceedings of the Chemical Process Control IV, 1991, pp. 271–296.
[27] K.H. Cheng, Q. Wang, J. Eur. Oper. Res. 97 (1997) 571–579.
[28] F. Zenith, PhD Thesis, Trondheim, Norwegian: Norwegian University of Science and Technology, 2007.
[29] J. Newman, K.E. Thomas-Alyea, Electrochemical Systems, 3nd ed., John Wiley & Sons, Chichester, 2004, pp. 212–213.
[30] Y.T. Qi, B. Huang, J.L. Luo, Chem. Eng. Sci. 61 (2006) 6057–6076.